Available online at www.sciencedirect.com
ScienceDirect
Solar Energy 81 (2007) 683–691
SOLAR ENERGY
www.elsevier.com/locate/solener

Hybrid ventilation in two interconnected rooms with a buoyancy source

R. Tovar [a,*], P.F. Linden [b], L.P. Thomas [c,1]

[a] Centro de Investigación en Energía, Universidad Nacional Autónoma de México, Apdo. Postal 34, Temixco Mor. 62580, Mexico
[b] Department of Mechanical and Aerospace Engineering, University of California San Diego, 9500 Gilman Drive, La Jolla, CA 920903-0411, USA
[c] Instituto de Física Arroyo Seco, Universidad Nacional del Centro, Pinto 399, 7000 Tandil, Argentina

Received 16 June 2005; received in revised form 5 July 2006; accepted 14 August 2006
Available online 16 October 2006

Communicated by: Associate Editor Matthias Santamouris

Abstract

The design of energy efficient buildings and the potential for using solar energy for heating and cooling is contingent upon optimizing the building ventilation systems. In this paper, we study the ventilation of two interconnected spaces, such as adjacent offices or areas in an open plan office. The goal is to locate return vents to increase the efficiency of night ventilation and to reduce energy consumption.

The flow in two interconnected rooms of similar sizes is studied experimentally using a tank divided by an interior vertical wall. A forced buoyancy source with a finite volume flux is located in the ceiling of one-room and an unforced vent is opened in the ceiling of the other room. The goal of the study is to understand the transient cooling/heating that occurs in this two-room system when a forced cold-air vent is located in the ceiling of the first room and a return ventilation exit is located in the second. In particular, we investigate the effects of varying the number of openings and their vertical positions in the interconnecting wall. First, a single opening at the bottom, middle or top of the shared wall is examined. Second, the case of two openings in the wall is considered, with the openings located at the top–bottom, top–middle, bottom–middle, and finally at two mid locations in the wall. The results are compared with the one-room case, which represents the reference case.

It was found that, irrespective of the number and locations of the openings, the flow evolves into a quasi-stationary stably stratified two-layer system, with the depths of the layers being different in each room. The average temperature inside each room initially decreases linearly with time and approaches the supply-air temperature at large times. This initial linear decrease holds until cold-air leaves the unforced room through the top-vent at time t_e. Subsequently, temperature decreases as an exponential function of time with a characteristic filling time $\tau = V/Q_s$, where V is the total volume of both rooms and Q_s is the source volume flux. The efficiency of the ventilation depends on the time t_e, and this depends, in turn, on an exchange flow that is established between the two-rooms by the differences in density in each room. For a single opening, the exchange flow takes place as a two-way flow in the opening, while for two openings the flow is from the forced room through the lower opening and in the opposite direction through the upper opening.

When the upper opening is located below the ceiling, this flow from the unforced room 'shields' the return vent from the dense fluid, thereby increasing the efficiency of the ventilation.

Keywords: Night ventilation; Two-rooms hybrid ventilation; Thermal stratification

1. Introduction

The energy consumed in cooling buildings is a major, and increasing, component of global energy usage, and a significant contributor to emissions of greenhouse gases. This energy consumption is used to provide internal comfort, both in terms of the temperature and quality of indoor air, using mechanical systems such as heaters and air conditioners. Conventional HVAC systems have significant energy demands. Furthermore, mechanically ventilated buildings can, in certain circumstances, have substantial negative effects on the health, productivity, and general

* Corresponding author.
E-mail address: rto@cie.unam.mx (R. Tovar).
[1] Researcher of CONICET.

0038-092X/$ - see front matter © 2006 Elsevier Ltd. All rights reserved.
doi:10.1016/j.solener.2006.08.009

Nomenclature

A_f	cross-section floor area of the forced room
A_u	cross-section floor area of the unforced room
B	buoyancy flux
g	acceleration due to gravity
H	height of the room
h	height of the wall opening from the bottom
h^*	dimensionless height
h_1, h_2	height of the interior openings from the bottom
Q_s	source volume flux
t	time
t^*	dimensionless time
T^*	dimensionless temperature
T_0	initial temperature
T_{avr}	average temperature
t_e	time when denser fluid leaves the unforced room through the top-vent
T_s	source temperature
V	total volume of both rooms
V_u	volume of the unforced room

Greek symbols

λ	entrainment constant for a buoyant plume
ρ^*	dimensionless density
ρ_{avr}	density averaged over the volume
ρ_s	density of the source salt solution
ρ_w	density of water
τ, τ_V	time to flush the space with the supply fluid
t_e, τ_u	time for the dense layer in the unforced room to reach the ceiling vent
τ_f, τ_{VH}	'filling-box' time
τ_{fh}	time for the dense layer in the forced room to reach a wall opening
τ_{uh}	time for the dense layer in the unforced room to reach the a wall opening
η	efficiency

Subscripts

0	initial value
avr	average
c	ceiling
e	exit
f	forced room, filling box
h, H	height
s	source
u	unforced room
V	volume
w	water

well-being of building occupants (Fisk, 2000). These problems will increase in importance as more countries adopt air-conditioning in new buildings.

The efficiency of a conventional overhead cooling system, in which cool supply air is introduced through overhead diffusers, is reduced if some of this cold-air leaves through return vents without cooling the space. For this reason returns are placed in the ceiling to reduce this loss of cooling capacity. Nevertheless, air flows within the space can cause cool air to reach the ceiling and the flow of supply air through the return leads to a loss of efficiency.

In this paper, we address the effect of locating the return vent in a space separated from, but connected to, the space with the supply vent. Such situations can occur in open plan spaces with internal partitions that may provide partial divisions of the space. These partitions can allow air to flow over and/or underneath them, thereby providing connections between the spaces at the top and the bottom. In some cases these partitions may be aligned with ceiling supports so that the openings occur at intermediate heights. Other situations that are relevant to this study are cases where offices are open to another space such as a corridor, so that cool air entering the office is extracted through a vent in the corridor.

In a closed space with both a supply and return vent in the ceiling, volume conservation implies that the flow rate leaving the return is the same as that entering through the supply. The aim of balancing a system is to ensure that this occurs even when there are alternative ways for air to leave or enter the space. The intent of an overhead supply is that the descending cold air provides kinetic energy to mix the space, so that the temperature is spatially uniform. Then the temperature of the air leaving the space is this average temperature. In displacement systems, where the supply is at floor level, stable stratification is promoted, and the return temperature is higher than the average room temperature.

Related work on buoyancy-driven flow in two interconnected rooms has been carried out by Wong and Griffiths (2001) and Lin and Linden (2002). A source of buoyancy in a 'forced room' was connected to another, finite volume 'unforced room' by one or more openings, but neither space is connected to the exterior and there is no ventilation of the building. Wong and Griffiths (2001) considered the simplest case of a single opening, and found two different behaviors depending on the vertical location of the opening. If the opening was located at the top of the room, buoyant fluid flowed out of the forced room into the unforced room, leading to the development of a buoyant layer in the unforced room extending from the ceiling to the bottom of the opening. The flow in the forced room develops in a very similar manner to the filling box. On the other hand, if the opening is at some distance below the ceiling, eventually buoyant fluid exits and rises as a turbulent plume in the other room. Filling-box type flows then

develop in both rooms, with exchange flow through the connecting opening.

Lin and Linden (2002) considered the qualitatively different circumstance where the two rooms, one larger than the other, were connected at both top and bottom levels. They found that the early-time evolution of the flow evolved through two distinct phases. Initially, displacement ventilation developed in the forced room with buoyant fluid flowing into the unforced room at high levels, and denser fluid flowing into the forced room at lower levels. Since the density distribution is continually evolving in the unforced room, it is not possible for the flow to approach a steady state. Instead, the system evolves on a time scale determined by the largest of the two-rooms.

In this paper, we present visualizations and detailed measurements for the transient evolution and the long-term flow. The flow regimes, the evolution of the average density and the stratification are studied in several geometrical configurations. The efficiency of the ventilation process is discussed in terms of the geometrical configurations and the flow patterns they produce.

We consider the applicability of this work to night purging of a building. In climatic zones where the diurnal temperature variation is sufficiently large and solar energy gains are unavoidable, low-energy buildings often employ night cooling to pre-condition the building to withstand the internal gains the following day, both to reduce the total cooling load and to shift the demand to an off-peak period, see, for instance, the work of Breesch et al. (2005). In the summer (the cooling season), cool outside air is flushed during the night through the building to extract heat from the building fabric.

We discuss the arrangement of supply and return vents to obtain the most efficient heat transport in an hybrid configuration that includes a mechanical device (such as a small fan) that introduces a volume flow of cool air through the forced vent. The dynamics of the interior flow is driven by buoyancy forces, caused by temperature differences, and the role of the fan is to introduce cool air into the building. The amount of energy transferred by the internal flow is much bigger than the energy consumed by the fan, so we can consider this arrangement as an active solar thermal system where the building acts as an energy storage.

2. Experimental set up

We carried out laboratory experiments and performed flow visualization in order to reveal the qualitative behavior of the flows and identify key processes which may not be easy to observe in real buildings. The laboratory experiments are conducted in water and have dynamical similarity with the full scale ventilation flows as described in Linden (1999). In the laboratory, the scale of each room is reduced by about a factor of about 10 compared with full scale. The model (0.60 m wide, 0.25 m high and 0.20 m deep) is filled with tap water ($\rho_w = 0.998$ g/cm^3), and doors and windows are simulated by rectangular openings which span the shared wall. These openings were 2.5 cm high for a single opening and 1.25 cm each when there were two openings. The openings spanned the full width of the wall, giving a total opening area 50 cm^2 in each case. A source of negative buoyancy is represented by a finite volume flux of fluid of different density (due to varying salt concentration) which flows through a nozzle designed to produce turbulent flow, Fig. 1.

The buoyancy source is located in the ceiling of one-room and an unforced vent is opened in the ceiling of the other room. The flow is produced by the injection of a salt solution ($\rho_s = 1.034$ g/cm^3) that generates a negatively buoyant turbulent plume, representing the flow from a cooling vent, inside the forced room. This plume is supplied with a buoyancy flux $B = gQ_s(\rho_s - \rho_w)/\rho_w$ and a finite volume flow rate $Q_s = 2.57$ cm^3/s^1 which is measured by a flow meter. The values of B and Q_s are constant during the experiments and are the same for all the cases. Due to volume conservation, this net volume flow rate is also established through the interconnecting openings between the rooms and through the external opening. The fluid released during an experiment is collected for later analysis; in particular, its volume and the elapsed time provide a check for the volume flow rate.

Dye is added to the salt water to provide flow visualization and to provide a non-intrusive means of measuring the density. A panel of florescent lights and a diffusive screen are located on one side of the model and a video camera on the other side (see Fig. 2). The images taken at different times by the camera are digitized and processed by *DigImage* software (Dalziel, 1995). The light absorbed by the dye is related to fluid density by means of a calibration (Cenedese and Dalziel (1998)). The values so obtained are averaged in small windows of the images centered in eleven vertical positions in both rooms. Since the light attenuation occurs across the tank, the vertical density profile is an across-tank average. At the end of an experiment the fluid contained in the model is mixed and its density measured by an Anton Paar DMA 5500 densimeter. This measurement confirms that the density measurements by image processing have less than 4% error. Shadowgraph images

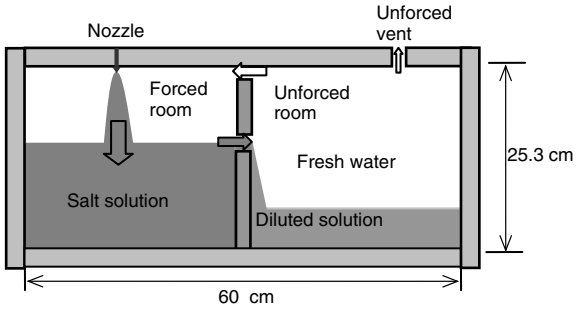

Fig. 1. Schematic view of the experimental model. Arrows represent direction and magnitude of the flows inside the model.

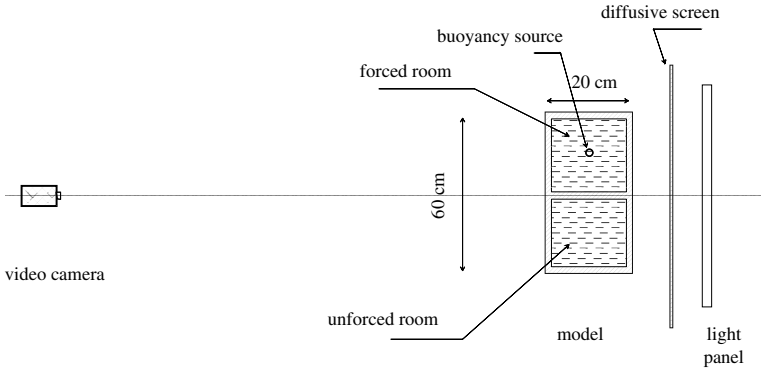

Fig. 2. Top view of the experimental set up for the whole-field density measurements.

are also used for qualitative purposes and to determine flow patterns.

3. Results

As a reference case for comparison we first describe the flow within a single space (Fig. 3a). Initially the space is at an initial density (associated with its initial temperature). As dense salt solution (cool air) enters it descends as a turbulent negatively-buoyant jet and spreads out along the floor producing a dense layer. The descending jet entrains fluid from within the room and its density decreases until it reaches the floor. As time progresses this dense layer rises as more dense salt solution is added. The jet at later times passes through and entrains some of this dense layer and so its density on reaching the floor is larger than at an earlier time. Consequently, increasingly dense fluid arrives at the floor and a stable stratification is established. This is the 'filling box' process described by Baines and Turner (1969) and by Caulfield and Woods (2002). During this stage, fluid with the initial density in the space is leaving from the upper vent at the same volume flow rate as it is supplied by the source. All of the salt solution added to the space remains in the tank at this point, and the volume-average density increases linearly with time.

This process continues until the initial dense layer reaches the upper vent. Now there is some loss of salt (cool air) from the upper vent. The flux is the local density at the vent multiplied by the supply flow rate. Since the latter is constant the loss of salt (cool air) is determined by the local concentration at the vent. As the 'filling box' process continues the salt concentration at the vent increases with time as the stratification is raised by the addition of denser fluid at the bottom of the tank. The time scale for this process is the 'filling-box' time $\tau_f = V/\lambda B^{1/3} H^{5/3}$, where V and H are the volume and height, respectively, of the space, and $\lambda \approx 0.1$ is the entrainment constant for the negatively buoyant plume. This time scale is the time required for all the fluid within the space to be recirculated through the plume.

However, even though there is loss of salt at the return vent, this is less than that supplied at the source. Consequently, the density within the tank increases, although now at a reducing rate, until eventually all the fluid within the tank has the same density (temperature) as the supply

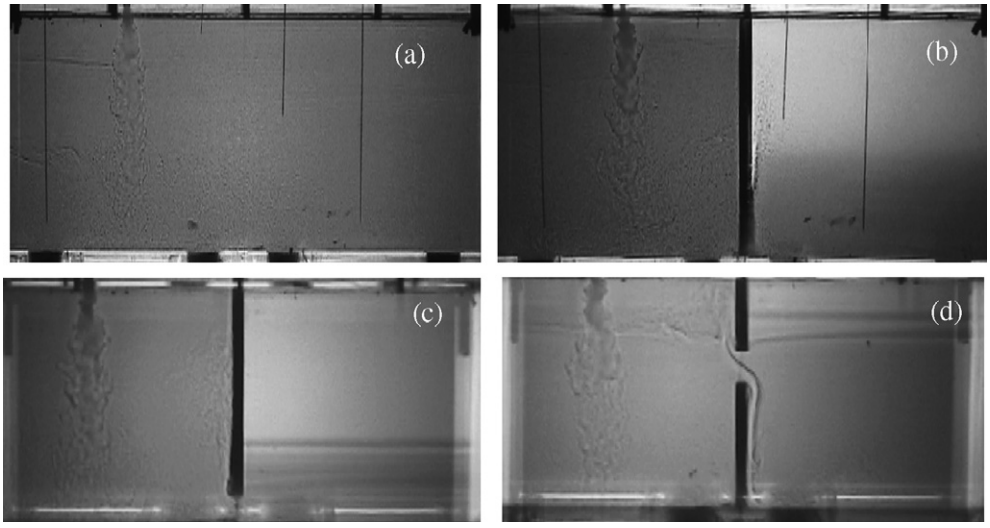

Fig. 3. Shadowgraph of the flow at $t = 1200$ s for the cases: (a) no interior wall (reference case), and single opening at the top (b), at the bottom (c) and the middle (d) of the shared wall. The exchange flow is not visible in (b) as the top of the tank obstructs the view.

fluid. At this point a steady state is reached. The time scale for this process is the time $\tau_V = V/Q_s$ required to flush the space with supply fluid, and $\tau_f \ll \tau_V$.

We now discuss the effects of placing a wall with openings between the source and the return vent on this evolution.

3.1. Flow in interconnected rooms with a single opening in the interior wall

The volume flow supplied by the source generates a flow from the forced chamber to the unforced chamber and from the unforced chamber via the return vent to the exterior of the tank. Initially, the plume spreads out along the floor of the forced room and creates a dense lower layer at the bottom. This bottom layer of dense fluid grows in depth until it reaches a wall opening at the filling-box time scale $\tau_{fh} = A_f h/\lambda B^{1/3} H^{5/3}$, where A_f is the area of the forced chamber and h is the height of the opening from the bottom. The filling box time scale is the time taken for all the fluid in the space to be entrained into the plume. It represents the characteristic time for the establishment of stratification in an unventilated space. For a single opening located at the top of the interior wall, the height of the opening is just the height of the chamber, $h \approx H$ (Fig. 3b).

After τ_{fh} a negatively buoyant layer descends as a turbulent wall plume in the unforced room creating there another dense layer of yet more diluted concentration. As time increases, the density in the forced room increases and the pressure difference across the opening also increases. Since this pressure difference is capable of driving a flow larger than the input flow Q_s, an exchange flow is established through the opening, with dense fluid flowing from the forced to the unforced chamber while less dense fluid flows in the opposite direction. The growing layer in the unforced room reaches the ceiling at the time t_e.

When the opening is at the top of the shared wall, the flow within the forced chamber develops as for a single chamber, as the interconnecting opening acts as a return vent for that space. Once the dense layer reaches the opening it then spills over into the other chamber and falls as a dense plume as shown in Fig. 3b. Since, in these experiments, the opening spans the full width of the room, this plume is a line plume and is attached to the wall as it descends. On reaching the floor it spreads out and a two-dimensional filling-box flow occurs in the unforced chamber. The pressure difference is observed to be large enough for an exchange flow to be established at this opening. As a consequence, some fresh water enters the forced chamber and is entrained into the source jet.

For an opening located at the bottom of the room, negatively buoyant fluid flows from the forced room into the unforced room from the beginning of the experiment. The development of a dense layer in the unforced room is associated with a high density gradient in the interface as seen in Fig. 3c. In this case, the exchange flow between both chambers occurs after the dense layer in the unforced chamber is deeper than the opening and the buoyant fluid of the unforced chamber does not enter the forced chamber. Even if there is an exchange flow through the opening, the depth of the dense layer in the unforced chamber increases only because of the fluid supplied by the source. The time t_e in which this layer reaches the ceiling is then given by $\tau_u = V_u/Q_s$, where V_u the volume in the unforced chamber.

An intermediate result is obtained if the opening is at an intermediate position between the ceiling and the floor (Fig. 3d). In this case, the time at which the dense fluid reaches the opening is $\tau_{fh} = A_f h/\lambda B^{1/3} H^{5/3}$, with $h < H$, after which time negatively buoyant fluid exits from the forced room and descends as a wall plume in the other room. Filling-box type flows then develop in the unforced room, with an exchange flow through the connecting opening. In this case, since the fluid entering the forced chamber is less dense it rises as a turbulent wall plume, and the exchange flow promotes mixing in both chambers. After the layer in the unforced room reaches the height of the opening, this entrainment stops and its growth rate decreases. The interface advances at a velocity given by the net volume supply of the source, and the negatively buoyant layer in the unforced room reaches the ceiling in an additional elapsed time $A_u(H - h)/Q_s$, where A_u is the cross-section area of the unforced room.

Therefore, the time t_e is specific for each case and depends on the height of the opening in the interior wall. It is different from the characteristic filling time $\tau = V/Q_s$, or the time given by the filling box model, $\tau_{VH} = V/\lambda B^{1/3} H^{5/3}$ of one-room without an internal wall.

3.2. Flow in interconnecting rooms with two openings in the interior wall

In this section, we present first the flow visualization and then we analyze the time evolutions of the average density. Measurements of the evolving density field are also presented.

When there are two openings the buoyancy-driven exchange flow that occurred in the single opening is separated between the two openings, so the flow in each opening is unidirectional. It is observed that in the lower opening the direction of the flow is always from the forced chamber to the unforced one, while in the upper opening the direction of the flow is in the opposite direction. We did not detect exchange flow in any opening in these experiments, probably because we had equal opening sizes. If there is a significant difference between the openings the physical situation may be closer to those described in Section 3.1, with exchange flow through the larger opening in such cases.

When the openings are located at the top and bottom of the room, the flow initially follows the process described in Lin and Linden (2002). On starting the source flow, there is an initial net flow Q_s from the forced chamber into the unforced chamber and out of the return vent.

Subsequently, an exchange flow between the two chambers is established as described above. The flow of dense fluid at the bottom and light fluid at the top causes little mixing and entrainment is important only in the plume generated by the source in the forced chamber. At later times the heavier layer in the unforced room rises and reaches the ceiling and then fluid, which is heavier than the initial ambient fluid, flows back into the top of the forced room and to the exterior. This flow of heavier fluid causes some additional mixing in the forced room.

A similar flow occurs when the openings are at intermediate heights. Again the flow from the forced chamber to the unforced chamber takes place through the lower opening, and the reverse flow takes place through the upper opening. Since the flow from the forced room is denser than that in the unforced room, this incoming flow falls as a turbulent wall plume (see Figs. 4b and d) while the flow from the unforced room rises as a turbulent wall plume when the opening is not at the top (see Figs. 4c and d). These plumes entrain fluid as they rise or fall producing a filling-box stratification in the two chambers.

Fig. 5 shows density profiles taken during the experiments shown in Figs. 4a and c, with the forced chamber shown in the panels on the left and the unforced chamber in the panels on the right. As expected, the density of each chamber increases with time and a stable stratification is established with the denser (cooler) fluid occurring at the floor of the chamber. In the case of the top–bottom combination (Fig. 5a) the stratification is largest in the forced chamber, due mainly to the inflow of less dense fluid from the unforced chamber through the top opening. Since this inflow occurs with little mixing, this leads to a significant reduction in density in the upper part of the forced chamber. On the other hand when the upper opening is moved down to a middle position (Fig. 5b) the larger stratification occurs in the unforced chamber. This is because, in this case, the upper part of the unforced chamber is 'shielded' from the dense layer rising from its base, as this fluid leaves through the middle opening into the forced chamber at later times.

The maximum densities in both chambers are, within experimental resolution, approximately the same. This reflects the fact that the openings are quite large so that only a small pressure difference is needed to establish the exchange flow. In both cases the neutral pressure level (the level where the pressure is the same in each chamber) lies between the two openings. Further, the densities are also approximately the same in the two cases at the same times. Thus the main effect of changing the opening positions is to change the strength of the stratification.

3.2.1. Mean density

The loss of dense fluid through the return vent implies that there is a loss of cooling from the system. We examine this loss by determining the total mass within the tank as a function of time. In the absence of any loss of dense fluid (i.e. only fresh water leaves through the upper return vent), the density ρ_{avr} averaged over the volume increases linearly with time. This can be expressed in dimensionless terms as

$$\rho^* = t^*, \tag{1}$$

where $\rho^* = (\rho_{avr} - \rho_0)/(\rho_s - \rho_0)$, $t^* = t/\tau$, and $\tau = V/Q_s$. The linear increase (1) will hold initially in all cases until some dense fluid reaches the level of the return vent.

After a time t_e mixed fluid will begin to be released from the tank and the mean density can evolve between two extreme possibilities, depending on the flow inside the tank. For an ideal displacement flow forming a two layer stratification with zero mixing, the mean density increases linearly according to (1) up to $\rho^* = 1$ at $t^* = 1$, when the density of the whole tank is the density of the source. This represents the most 'efficient' system with zero loss of cooling power.

At the other extreme, the least efficient case occurs when there is instantaneous and complete mixing in the whole

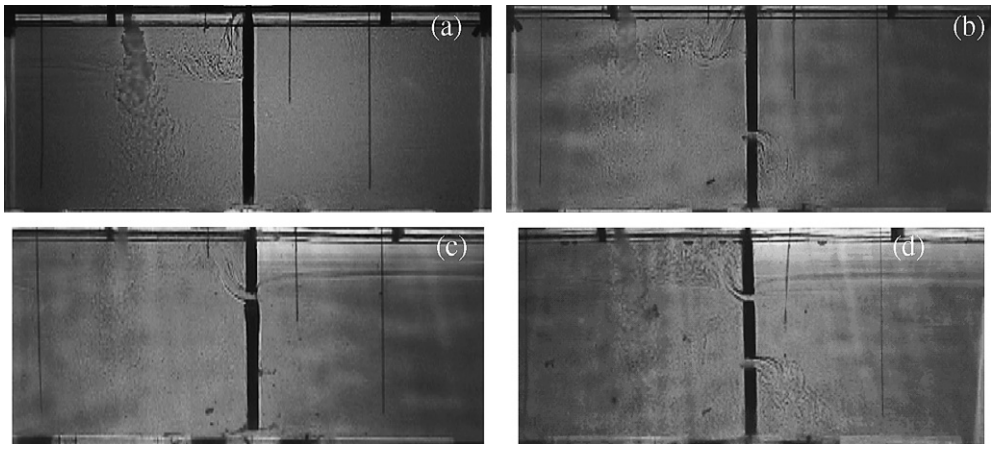

Fig. 4. Shadowgraph images of the flow with two openings in the interior wall at 1200 s. The forced room is on the left and the unforced room is on the right: (a) top–bottom; (b) top–medium; (c) medium–bottom; and (d) medium–medium.

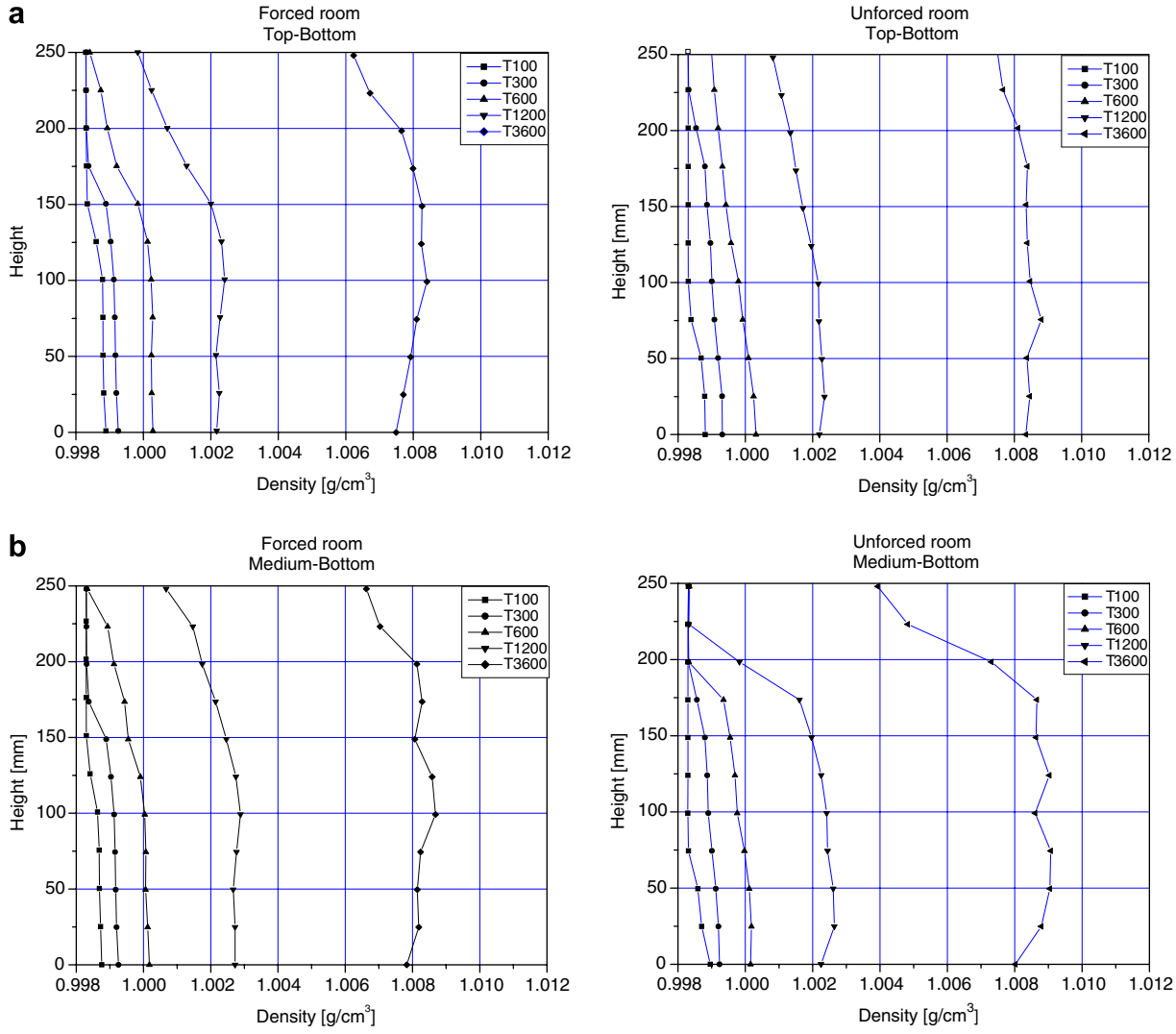

Fig. 5. Density profiles measured in a model with two openings in the interior wall for: (a) top–bottom and (b) medium–bottom configurations. The figures on the left correspond to the forced room while the figures on the right are for the unforced room. The times in the legend are the elapsed time in seconds since the start of the experiment.

volume from the beginning of the experiment ($t = 0$), the average density is $\rho_{avr} = \rho$ and is given by the balance

$$V\frac{d\rho}{dt} = Q_s(\rho_s - \rho). \tag{2}$$

Integrating (2) from $t = 0$ and applying the non-dimensionalization gives

$$\rho^* = 1 - e^{-t^*}. \tag{3}$$

In this case the density approaches the supply density ($\rho^* = 1$) exponentially in the limit $t^* \to \infty$. After one replenishment time, $t^* = 1$, the average density in this case is $\rho^* = 0.632$, representing a loss of about 37% of the input cooling power. In terms of temperature, (1) and (3) may be written respectively as $T^* = t^*$ and $T^* = 1 - e^{-t^*}$, where $T^* = (T_{avr} - T_0)/(T_s - T_0)$.

Fig. 6 shows the average density evolution for the same experiments shown in Figs. 4a and c. In the top–bottom configuration, the presence of the interior wall and the extreme locations of the openings induce high mixing due to the global recirculation in both rooms from the beginning of the experiments. Weak stratification is developed in the forced room and density in the unforced room is homogeneous, as seen in Fig. 5. In this case the mean density evolves the closest to the well-mixed model. The lowest efficiency compared with the no-mixing model is achieved in this case.

The effect of having a small interior wall attached to the ceiling not only delays the arrival of the unforced room buoyancy-layer to the unforced vent, but also allows a high density gradient to develop in that region. As will see in the next section, efficiency notably increases as compared with the top–bottom case.

We define the efficiency of the ventilation as

$$\eta = \frac{\rho^* - 1 + e^{-t^*}}{t^* - 1 + e^{-t^*}}, \tag{4}$$

so that the unmixed displacement case corresponds to $\eta = 1$, and the well-mixed case has an efficiency $\eta = 0$.

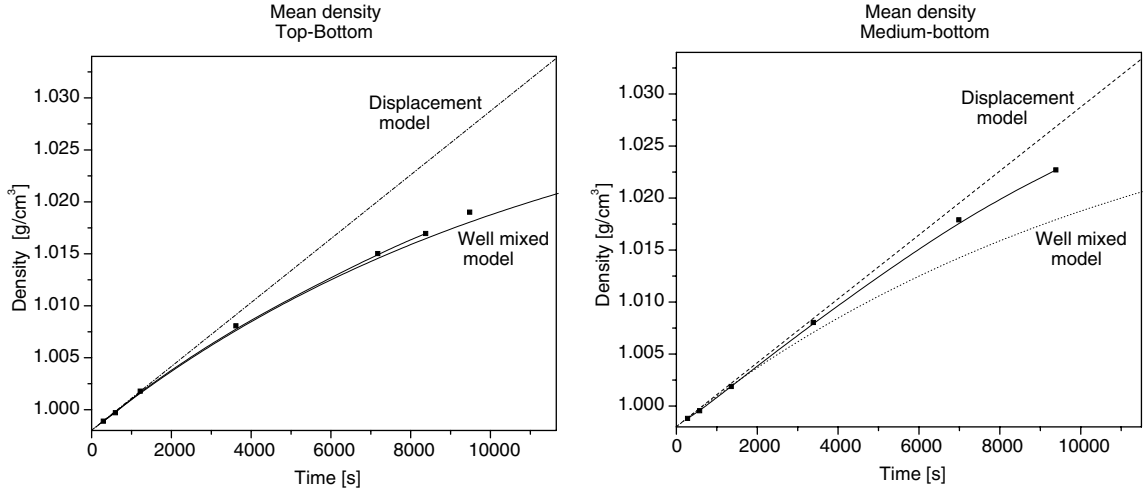

Fig. 6. Evolution of the average density inside the model for the top–bottom and the medium–bottom configurations.

Table 1
Efficiency and stratification for the cases studied measured at $t^* = 0.62$

Configuration	η (%)	Layers arrival times (s)				Stratification (g cm^{-3})
		Forced room τ_{fh}, τ_{fc}		Unforced room τ_{uh}, t_e		
		Wall opening	Ceiling	Wall opening	Ceiling vent	
Bottom $h^* = h/H = 0$	71	10	360	10	4500	0.0110
Medium $h^* = 0.57$	71	70	500	400	1960	0.0073
Top $h^* = 0.9$	50	300		1500	1500	0.0086
		Lower opening		Upper opening		
Bottom–medium $h_1^* = 0$, $h_2^* = 0.62$	57	10	300	200	1800	0.0060
Medium–medium $h_1^* = 0.33$, $h_2^* = 0.62$	50	15	300	200	1800	0.0074
One-room	32	–	660	–	660	0.0063
Medium–top $h_1^* = 0.33$, $h_2^* = 0.95$	21	25	540	330	450	0.0030
Top–bottom $h_1^* = 0$, $h_2^* = 0.95$	3.5	10	450	320	450	0.0035

Thus the efficiency depends on time, and, most importantly, on the strength of the stratification, which depends on the flow regime developed in each configuration, i.e. on the relative locations and number of the openings.

In Table 1 both the total stratification, defined as the density difference between the lower layer of the forced room and the upper layer of the unforced room, and the efficiency for each configuration of the system for time $t^* \approx 1 - e^{-1} = 0.63$ are presented. Indeed, at this time, for the well mixed model, loss of cooling power is ≈25%, and the instantaneous efficiency is $d\rho^*/dt^* \approx 0.5$.

4. Conclusions

This paper describes laboratory experiments that investigate the behavior of two interconnected rooms subject to a supply of cool air in one-room and a return vent in a second-room. The effects of different locations of the openings in the shared wall between the two-rooms on the flow patterns, the thermal stratification and the efficiency of the cooling have been studied. The experiments are conducted in water and the supply of cool air is represented by the addition of salt solution at a given concentration. Measurements are made of the salt concentration, and these are directly equivalent to the air temperature within a space. Further, since density differences are small compared with the mean density the Boussinesq approximation is valid and these flows are also equivalent to, but inverted from, that of a supply of warm air from a vent in the floor and a return vent also located in the floor as is found in some underfloor systems.

In night cooling the inclusion of a mechanical device (such as a small fan) to produce this kind of hybrid system, is recommended when there is not enough stack effect to drive the flow through the building. The transient response is directly applicable, since the maximum cooling is required in the shortest time to reduce the consumption of fan energy.

A conventional overhead cooling system is designed to produce a space at a uniform temperature. Since the loss of cooling capacity is determined by the amount of cold-air that leaves the return vent, this is the most inefficient when the space is well-mixed. Our measurements of a single space show that, in practice, because some stratification

inevitably occurs, the efficiency is higher than this well-mixed minimum.

When there are partial barriers between the supply vent and the return, the efficiency increases as the flow of cold-air towards the return vent is inhibited by the flow patterns established within the space. Significantly, the openings between the rooms are large in the sense that they do not block the flow Q_s from the source, and the small pressure drops necessary to drive flows between the two chambers are easily established by small differences in temperatures between them. Thus we observe large internal flows that are organized by the locations of the openings. It is these internal flows that stop the cool air from reaching the return vent and thereby increase the efficiency of the ventilation.

In the case of a single opening, the internal flow takes the form of a two-way exchange flow in the opening. When there are two (or more) openings, this exchange flow is separated between the openings. The most efficient cases are those where there is no opening near the top of the wall. In this case the region underneath the return vent in the unforced room remains relatively isolated for a long time, so that the warmest air in the space is near the return vent.

The main conclusion of this study is that the presence of partial barriers to flow within a room can lead to significant internal flows, with consequent differences in the exchange of heat through vents open to the exterior. We show that 'shielding' an upper vent from cool air by a vertical barrier at the ceiling can significantly reduce the rate of loss of cooling from a space. The addition of such barriers may, therefore make low-energy options such as night cooling a viable option for cooling a building.

Acknowledgments

The authors acknowledge the partial support of CONACYT project U41347-F. R. Tovar was supported by UC-MEXUS CONACYT, Grant 6925, and by DGAPA-UNAM.

References

Baines, W.D., Turner, J.S., 1969. Turbulent buoyant convection from a source in a connected region. J. Fluid Mech. 37, 51–80.

Breesch, H., Bossaer, A., Janssens, A., 2005. Passive cooling in a low-energy office building. Sol. Energy 79, 682–696.

Caulfield, C.P., Woods, A.W., 2002. The mixing in a room by a localized finite-mass-flux source of buoyancy. J. Fluid Mech. 471, 33–50.

Cenedese, C., Dalziel, S.B., 1998. Concentration and depth field determined by the light transmitted through a dyed solution. In: Proceedings of the Eighth International Symposium on Flow Visualization, pp. 61.1– 61.5.

Dalziel, S.B., 1995. DigImage: System Overview. Cambridge Environmental Research Consultants, Cambridge, UK.

Fisk, W.J., 2000. Health and productivity gains from better indoor environments and their relationship with building energy efficiency. Ann. Rev. Energy Environ. 25, 537–566.

Lin, Y.J.P., Linden, P.F., 2002. Buoyancy-driven ventilation between two chambers. J. Fluid Mech. 463, 293–312.

Linden, P.F., 1999. The fluid mechanics of natural ventilation. Ann. Rev. Fluid Mech. 31, 201–238.

Wong, A.B.D., Griffiths, R.W., 2001. Two-basin filling boxes. J. Geophys. Res. 106 (C11), 26929–26941.